



**HAL**  
open science

# Estimation of Earth interior parameters from a Bayesian inversion of very long baseline interferometry nutation time series

L. Koot, A. Rivoldini, O. de Viron, V. Dehant

## ► To cite this version:

L. Koot, A. Rivoldini, O. de Viron, V. Dehant. Estimation of Earth interior parameters from a Bayesian inversion of very long baseline interferometry nutation time series. *Journal of Geophysical Research: Solid Earth*, 2008, 113, 10.1029/2007JB005409 . insu-03603712

**HAL Id: insu-03603712**

**<https://insu.hal.science/insu-03603712>**

Submitted on 10 Mar 2022

**HAL** is a multi-disciplinary open access archive for the deposit and dissemination of scientific research documents, whether they are published or not. The documents may come from teaching and research institutions in France or abroad, or from public or private research centers.

L'archive ouverte pluridisciplinaire **HAL**, est destinée au dépôt et à la diffusion de documents scientifiques de niveau recherche, publiés ou non, émanant des établissements d'enseignement et de recherche français ou étrangers, des laboratoires publics ou privés.

Copyright

## Estimation of Earth interior parameters from a Bayesian inversion of very long baseline interferometry nutation time series

L. Koot,<sup>1</sup> A. Rivoldini,<sup>1</sup> O. de Viron,<sup>2</sup> and V. Dehant<sup>1</sup>

Received 27 September 2007; revised 1 February 2008; accepted 27 March 2008; published 22 August 2008.

[1] Among the variations in the rotation of the Earth, the nutation is the most suitable for studying the Earth's internal structure. The nutation is mainly driven by the gravitational torque of the Moon, the Sun and the planets acting on its equatorial bulge. The Earth response to this external forcing is influenced by its internal structure. Because the gravitational forcing is known to a very good accuracy, the high precision nutation observations, using the very long baseline interferometry (VLBI) technique, allow to estimate Earth interior parameters. The nutational response of the nonrigid Earth to the gravitational forcing has previously been modeled by a semianalytic model which depends on parameters, related to the Earth interior, that are adjusted on the nutation observations. Those parameters are the dynamical ellipticities of the whole Earth and fluid core, compliances describing the deformability of the whole Earth and fluid core, and coupling constants related to the torques generated by the differential rotation of the mantle, fluid core and solid inner core. Most of the nutation models are frequency domain models so that, in previous studies, the time series of observations are processed before the fit in order to get data in the frequency domain. Because the parameters are fit only on the twenty dominant terms in the frequency domain, this fit leads to a loss of information. In this paper, we present a new fit procedure of the nutation model to the observations, which estimates the Earth's parameters directly from the time series of nutation data. This allows to use all the information of the time domain data and to account for the time variable uncertainties on the data (this time variability is due to the improvement of the measurement techniques). Rather than the linearized least squares method used in previous studies, we use a probabilistic (Bayesian) inversion method. This method does not rely on the assumption that the model is linear in its parameters, it is thus particularly well-suited for the highly nonlinear nutation model. In addition, we include an additional parameter to allow for uncertainties in the nutation model itself. This parameter is estimated jointly with the geophysical parameters. As result, we obtain a probability distribution on the parameters. The numerical results are compared with those obtained from previous studies.

**Citation:** Koot, L., A. Rivoldini, O. de Viron, and V. Dehant (2008), Estimation of Earth interior parameters from a Bayesian inversion of very long baseline interferometry nutation time series, *J. Geophys. Res.*, *113*, B08414, doi:10.1029/2007JB005409.

### 1. Introduction

[2] Earth's rotation variations can be separated into three components: the polar motion, length-of-day variations and the nutation. While the polar motion and length-of-day variations are mostly driven by the effects of the external geophysical fluids (atmosphere, ocean and hydrology), nutation on the other hand is mainly driven by the external gravitational forcing from the Sun, the Moon and, to a lesser extent, the other planets of the solar system. The rotational

response of the Earth to those external geophysical and gravitational forcings depends on its internal structure. The forcing of the polar motion and length-of-day variations by the geophysical fluid layers is poorly determined. On the other hand, as the positions of the celestial bodies are known very accurately from the ephemerides, the gravitational forcing, acting on the Earth and giving rise to nutation, can be computed very precisely. This explains the interest of studying the nutation: the forcing being well known, the comparison of the nutation model with the observations allows to get information on the Earth's internal structure.

[3] Classically, the nutation for the nonrigid Earth is modeled in two steps. First, from the gravitational torque exerted by the Sun, Moon and planets, the nutation of an hypothetical rigid and homogeneous Earth is computed. Then, the rigid-Earth nutation motion is convolved with a transfer function, which contains the departures of the real

<sup>1</sup>Department of Reference Systems and Geodynamics, Royal Observatory of Belgium, Brussels, Belgium.

<sup>2</sup>Institut de Physique du Globe de Paris, associé au CNRS et à l'Université de Paris VII, Paris, France.

Earth from the rigid and homogeneous approximation. All the geophysical modeling of the Earth internal structure is included in this transfer function. This two-step procedure allows to separate the geophysical aspects concerning the Earth's interior from the celestial mechanics problem of the rigid Earth nutation.

[4] The transfer function for the nonrigid Earth adopted by the International Astronomical Union (IAU) since 2000 is based on the model developed by *Mathews et al.* [2002]. In the following, this paper will be referred to as MHB. The model derived in MHB is semianalytic: the analytic equations depend on several parameters, characterizing the internal structure, which are computed numerically. Among these parameters, those that have a large influence on the nutational response of the Earth are fit on the nutation observations.

[5] As the gravitational forcing of nutation can, to a very good degree of approximation, be decomposed as a sum of periodic terms, nutation models are often built in the frequency domain. On the other hand, nutation observations are given as time series. In order to fit the model to the observations, the method used in the IAU2000 model [*Herring et al.*, 2002] consists in estimating from the data, with the least squares method, the complex amplitude of the prograde and retrograde part of each periodic term, whose frequencies are known from the rigid-Earth nutation theory. They estimate the complex amplitudes of 21 frequencies in the nutation series. The specific terms chosen are those that can be reliably estimated (some of the nutation frequencies are so close that a reliable estimate of the associated amplitudes is unachievable). However, those nearby frequency terms, which could not be estimated separately, were taken into account in the computation. The secular trends, corresponding to a change in the precession constant and an obliquity rate, are also estimated. The geophysical parameters of the nutation model are then adjusted to these complex amplitudes and to the precession rate with a linearized least squares method.

[6] In this paper, we develop a new method to estimate the Earth internal parameters from nutation observations. First, rather than to process the data to get frequencial information, we express the nutation model in time domain in order to be able to adjust it directly to the time series data. This avoids the loss of information due to the truncation at the 21st term in the frequency domain. The quality of the nutation data is varying in time due to the improvement of the measuring techniques. A processing of the data in the time domain allows to take directly this time variation of the quality into account. Note however that the time dependent data quality was also taken into account by *Herring et al.* [2002] when computing the complex amplitudes at given frequencies. The procedure presented here allows to remove this intermediate step and allows for a direct estimation of the Earth interior parameters from the data time series.

[7] We use Bayesian inversion to estimate the parameters from the data in the time domain. The main reason is that the linearized least squares fit, used in IAU2000, is only justified if the dependence of the model in its parameters is weakly nonlinear. This assumption is not satisfied by the nutation model which has a highly nonlinear dependence in its parameters. The results are probability distributions on

the parameters, which is more general than a single numerical value and an associated error on the parameter.

[8] Finally, we include in the Bayesian framework modeling uncertainties accounting for some imperfections in the nutation model itself. Imperfections in the model may arise from the following causes: the Earth's interior model is very simple, the effects of ocean tides on nutation are computed by using ocean models which assimilate some oceanic data, and the atmospheric excitation of nutation is poorly known.

[9] We notice here that another estimation of Earth internal parameters from VLBI nutation time series has been recently performed by *Krasinski and Vasilyev* [2006]. This estimation relies on the theoretical model of *Krasinski* [2006] (note that P. M. Mathews, N. Capitaine, and V. Dehant proposed a comment to this paper, available on arXiv, DOI:2007arXiv0710.0166M). However, *Krasinski and Vasilyev* [2006] did not estimate the same parameters, what does not allow for a direct comparison with our results.

## 2. Nutation Model

### 2.1. Dynamical Equations

[10] The Earth's interior model used by MHB is made of three ellipsoidal layers: the anelastic mantle, the liquid outer core and the solid inner core. These layers interact with each others because of pressures on the boundaries, gravitational, electromagnetic and viscous couplings. The pressure coupling is separated into a contribution coming from the ellipsoidal shape of the boundaries, which is called the inertial coupling, and a contribution from the additional topography of the interfaces, which is called the topographic coupling. The rotation of the Earth is perturbed by an external tidal potential, which creates a torque  $\Gamma$  on the Earth's equatorial bulge.

[11] Each region within the Earth has an instantaneous rotation vector:  $\Omega$  for the whole Earth,  $\Omega_f$  and  $\Omega_s$  for the outer and inner cores respectively. The rotation of the three-layered Earth is derived from the angular momentum budget equations which relates the angular momentum of the whole Earth  $\mathbf{H}$ , the fluid core  $\mathbf{H}_f$  and the solid inner core  $\mathbf{H}_s$  to the torques applied on these regions. From *Mathews et al.* [1991a, 1991b] and MHB, those equations can be written as:

$$\begin{cases} \frac{d\mathbf{H}}{dt} + \Omega \times \mathbf{H} = \Gamma \\ \frac{d\mathbf{H}_f}{dt} + \Omega \times \mathbf{H}_f = \Omega_f \times \mathbf{H}_f + \Gamma^{CMB} - \Gamma^{ICB} \\ \frac{d\mathbf{H}_s}{dt} + \Omega \times \mathbf{H}_s = \Gamma_s + \Gamma^{ICB}. \end{cases} \quad (1)$$

[12] The torque  $\Gamma_s$  on the inner core is the sum of three contributions: the gravitational torque generated by the external tidal potential, the gravitational torque generated by the masses in the mantle and fluid core and the torque which results from the fluid pressures acting on the ellipsoidal surface of the inner core. This torque has been computed by *Mathews et al.* [1991a, 1991b]. The torque  $\Gamma^{ICB}$  results from all the other types of interactions between the layers (electromagnetic, viscous, topographic) which can create a torque on the inner core. In the same way,

the torque  $\Gamma^{CMB}$  results from all such couplings applied on the fluid outer core.

[13] The instantaneous rotation vector can be expressed in terms of the so-called wobbles of the mantle  $\mathbf{m}$ , fluid outer core  $\mathbf{m}^f$  and solid inner core  $\mathbf{m}^s$ . They are defined by:  $\Omega = \Omega_0 (\mathbf{i}_3 + \mathbf{m})$ ,  $\Omega^f = \Omega_0 (\mathbf{i}_3 + \mathbf{m} + \mathbf{m}^f)$  and  $\Omega^s = \Omega_0 (\mathbf{i}_3 + \mathbf{m} + \mathbf{m}^s)$ , where  $\Omega_0$  is the mean rotation rate of the Earth and  $\mathbf{i}_3$  is the instantaneous figure axis.

[14] In order to study nutation, only the two first components of the three-dimensional vectorial equation (1) are of interest and it is conventional to introduce complex combination of these two first components, e.g.,  $\tilde{m} = m_1 + im_2$ .

[15] The angular momentum for each layer appearing in equation (1) can be written as the product of its inertia tensor and its instantaneous rotation vector. The inertia tensor of each layer is composed of the principal moments of inertia of that layer in the equatorial plane ( $A$ ,  $A^f$ ,  $A^s$ , respectively for the whole Earth, outer and inner cores) and axial direction ( $C$ ,  $C^f$ ,  $C^s$ ) and of small corrections,  $c_{ij}$ ,  $c_{ij}^f$  and  $c_{ij}^s$ , which arise from the deformation of the Earth, of the outer core and of the inner core respectively. Those deformations are the consequence of the tidal potential and the centrifugal potentials of the whole Earth, fluid outer and solid inner cores. Following *Sasao et al.* [1980], the increments to the inertia tensors due to the deformations can be expressed as a linear combination of the parameters characterizing the deformation ( $\tilde{\phi}$ , the nondimensional tidal potential introduced by *Mathews et al.* [1991a, 1991b], for the tidal deformations and  $\tilde{m}$ ,  $\tilde{m}^f$  and  $\tilde{m}^s$  for the deformations due to the centrifugal potential of the Earth, outer and inner cores respectively):

$$\begin{cases} \tilde{c}_3 \equiv c_{31} + ic_{32} = A[\kappa(\tilde{m} - \tilde{\phi}) + \xi\tilde{m}_f + \zeta\tilde{m}_s] \\ \tilde{c}_3^f \equiv c_{31}^f + ic_{32}^f = A^f[\gamma(\tilde{m} - \tilde{\phi}) + \beta\tilde{m}_f + \delta\tilde{m}_s] \\ \tilde{c}_3^s \equiv c_{31}^s + ic_{32}^s = A^s[\theta(\tilde{m} - \tilde{\phi}) + \chi\tilde{m}_f + \nu\tilde{m}_s]. \end{cases} \quad (2)$$

where the parameters  $\kappa$ ,  $\gamma$ ,  $\theta$ ,  $\xi$ ,  $\beta$ ,  $\chi$ ,  $\zeta$ ,  $\delta$  and  $\nu$  are called the compliances. Those parameters describes the ability of the different regions of the Earth to deform due to different causes. They can also be written in terms of the Love numbers. Because of the anelasticity of the mantle, there is a phase lag between the tidal forcing and the deformational response. Within this setting, the compliances become complex and frequency dependent. However, when studying nutation, only diurnal variations are of interest so that, in the narrow band of the nearly diurnal frequencies, the compliances can be considered as constant in the frequency band of nutations.

[16] In the MHB nutation model, the dynamical equation (1) are expanded to first order in the perturbation. Because the tidal torque  $\Gamma$ , or equivalently the nondimensional quantity  $\tilde{\phi}$ , can be expressed very accurately as the sum of periodic terms with frequency  $\sigma$ , the linearized dynamical equations can be solved for each frequency independently.

[17] By expanding the dynamical equation (1) to the first order and expressing the angular momentum in terms of the wobbles and inertia tensors (whose increments due to deformations are given by equation (2)), those equations can be written in the following matricial form:

$$\mathbf{M}(\mathbf{g}, \sigma)\mathbf{x}(\sigma) = \tilde{\phi}(\sigma)\mathbf{y}(\mathbf{g}, \sigma), \quad (3)$$

where  $\mathbf{x}$  is the 4-dimensional vector defined by:

$$\mathbf{x}(\sigma) = \begin{pmatrix} \tilde{m}(\sigma) \\ \tilde{m}^f(\sigma) \\ \tilde{m}^s(\sigma) \\ \tilde{n}^s(\sigma) \end{pmatrix} \quad (4)$$

$\mathbf{M}$  is a  $4 \times 4$  matrix and  $\mathbf{y}$  is a 4-dimensional vector whose complete expressions are given by *Mathews et al.* [1991a, 1991b, equations (26b)–(26c)] and in MHB for the contributions arising from the torques  $\Gamma^{CMB}$  and  $\Gamma^{ICB}$ . The fourth equation of the system in equation (3) comes from the freedom of motion of the solid inner core in its fluid environment which effect has to be added to equation (1) in order to completely describe the rotation of the three-layered Earth model. This equation, derived in *Mathews et al.* [1991a, 1991b], is a function of  $\tilde{n}^s$ , the tilt of the solid inner core with respect to the mantle.

[18] The parameter  $\mathbf{g}$  introduced in equation (3) contains all the geophysical parameters of the Earth interior model, namely, the dynamical ellipticities of each region, defined as  $e \equiv (C - A)/A$  for the whole Earth and equivalently for the outer and inner cores, the nine compliances introduced in equation (2) and two nondimensional complex constants,  $K^{CMB}$  and  $K^{ICB}$ , related to the torques  $\Gamma^{CMB}$  and  $\Gamma^{ICB}$  by the following relations:

$$\begin{cases} K^{CMB} = \tilde{\Gamma}^{CMB} / (i\Omega_0^2 A^f \tilde{m}^f) \\ K^{ICB} = \tilde{\Gamma}^{ICB} / (i\Omega_0^2 A^s (\tilde{m}^s - \tilde{m}^f)) \end{cases} \quad (5)$$

They are referred to hereafter as the coupling constants at the CMB and the ICB.

[19] Using Euler's kinematic relation, which in the frequency domain can be expressed as:

$$\tilde{\eta}(\sigma) = -\frac{\tilde{m}(\sigma)}{1 + \sigma}, \quad (6)$$

the solution for the complex nutation  $\tilde{\eta}$  can be computed from the solution of the mantle wobble  $\tilde{m}$  obtained with equation (3) by inverting the matrix  $\mathbf{M}$  for each value of the frequency:

$$\tilde{\eta}(\mathbf{g}, \sigma) = -\frac{[\mathbf{M}^{-1}(\mathbf{g}, \sigma)\mathbf{y}(\mathbf{g}, \sigma)]_1 \tilde{\phi}(\sigma)}{1 + \sigma} \quad (7)$$

where  $[\dots]_1$  stands for the first component of the 4-vector and  $\mathbf{M}^{-1}$  the inverse of  $\mathbf{M}$ . The complex nutation  $\tilde{\eta}$  appearing in equations (6) and (7) is defined by  $\tilde{\eta} = \Delta\psi \sin \epsilon_0 + i\Delta\epsilon$ , where  $\Delta\psi$  and  $\Delta\epsilon$  are the components of the nutation in longitude and in obliquity respectively.

[20] Instead of expressing the nutation as a function of the gravitational potential  $\tilde{\phi}$  as it is done in equation (7), the effect of the gravitational potential on a hypothetical rigid and homogeneous Earth is computed, and the nutation of the nonrigid Earth is expressed in terms of the rigid Earth nutation. It can be shown [*Mathews et al.*, 1991a, 1991b; MHB] that the first order equations for the nutation of the

nonrigid Earth can be written as the product of the rigid Earth nutation  $\tilde{\eta}_R$  and a transfer function:

$$\tilde{\eta}(\mathbf{g}, \sigma) = \frac{e_R - \sigma}{e_R} [\mathbf{M}^{-1}(\mathbf{g}, \sigma) \cdot \mathbf{y}(\mathbf{g}, \sigma)]_1 \tilde{\eta}_R(\sigma, e_R), \quad (8)$$

where  $e_R$  is the value of the dynamical ellipticity used in the rigid-Earth model, which can be different from the one used in the nonrigid model (contained in the set of parameters  $\mathbf{g}$ ).

[21] Several rigid-Earth nutation models have been devised and they all reach a very high accuracy (of the order of 0.1  $\mu$ as). In this work, we use the rigid-Earth model RDAN97 developed by *Roosbeek and Dehant* [1998]. Their value of  $H_d = 0.0032737674$  leads to  $e_R = 0.0032845202$ .

## 2.2. Ocean Tides Effects

### 2.2.1. Modification of the Dynamical Equations

[22] Ocean tides modify the nutational response of the Earth for two reasons: they induce increments in the inertia tensors and change the angular momentum balance due to the motion of the water with respect to the Earth surface. The increment to the inertia tensor of the whole Earth due to the ocean tides is written  $\tilde{c}_3^O$  and is due to the additional ocean mass itself and to the load induced deformation. The increment to the inertia tensor of the fluid core,  $\tilde{c}_3^{FO}$ , is due to the load induced deformations of the fluid core. Strictly speaking, there would also be an increment to the inertia tensor of the solid inner core, but this effect is very small and consequently is neglected. Therefore the ocean tides contribution to nutation can be studied in the framework of the two-layered Earth model used by *Sasao and Wahr* [1981].

[23] The increments  $\tilde{c}_3^O$  and  $\tilde{c}_3^{FO}$  can be expressed, according to *Sasao and Wahr* [1981], in terms of a dimensionless potential  $\tilde{\phi}_L$  resulting from the surface load and of three parameters  $\tau$ ,  $\chi$  and  $\eta$ . The surface load potential induces two kinds of increments in the inertia tensor of the whole Earth. The first one is an increment resulting from the loading mass of the ocean itself and can be described by the parameter  $\tau$ :

$$\tilde{c}_3^M = -A\tau\tilde{\phi}_L. \quad (9)$$

The second increment is due to the deformation of the Earth induced by the loading mass and is described by the parameter  $\chi$ . The total increment in the inertia tensor of the whole Earth due to the surface load potential can then be written:

$$\tilde{c}_3^O = -A(\tau - \chi)\tilde{\phi}_L \quad (10)$$

The increment to the inertia tensor of the fluid core, due to the load-induced deformation, is described by the parameter  $\eta$ :

$$\tilde{c}_3^{FO} = A\eta\tilde{\phi}_L \quad (11)$$

[24] By putting the increments to the inertia tensors  $\tilde{c}_3^O$  and  $\tilde{c}_3^{FO}$  as well as the relative angular momentum of the ocean  $\tilde{H}$  in the dynamical equations, we get:

$$\mathbf{M}(\mathbf{g}, \sigma)\mathbf{x}(\sigma) = \mathbf{y}(\mathbf{g}, \sigma)\tilde{\phi}(\sigma) + \mathbf{y}_c(\sigma)\frac{\tilde{c}_3^O(\sigma)}{A} + \mathbf{y}_h(\sigma)\frac{\tilde{h}(\sigma)}{A\Omega_0} \quad (12)$$

where the first term of the right-hand-side, representing the gravitational forcing, is the same as in equation (3), and where:

$$\mathbf{y}_c(\sigma) = \begin{pmatrix} -(1 + \sigma) \\ \sigma \frac{\eta}{\tau - \chi} \\ 0 \\ 0 \end{pmatrix} \text{ and } \mathbf{y}_h(\sigma) = \begin{pmatrix} -(1 + \sigma) \\ 0 \\ 0 \\ 0 \end{pmatrix} \quad (13)$$

[25] With the modified dynamical equations given in equation (12), one obtains the nutation amplitude of a three-layered Earth with ocean tides:

$$\tilde{\eta}(\mathbf{g}, \sigma) = \frac{e_R - \sigma}{e_R} [\mathbf{M}^{-1}(\mathbf{g}, \sigma) \cdot \mathbf{y}(\mathbf{g}, \sigma)]_1 \tilde{\eta}_R(\sigma, e_R) - \frac{[\mathbf{M}^{-1}(\mathbf{g}, \sigma) \cdot \mathbf{y}_c(\sigma)]_1}{1 + \sigma} \frac{\tilde{c}_3^O(\sigma)}{A} - \frac{[\mathbf{M}^{-1}(\mathbf{g}, \sigma) \cdot \mathbf{y}_h(\sigma)]_1}{1 + \sigma} \frac{\tilde{h}(\sigma)}{A\Omega_0} \quad (14)$$

where, again, the first term represents the gravitational forcing and is the same as in equation (8).

### 2.2.2. Computation of $\tilde{c}_3^O$ and $\tilde{h}$ From OTAM Data

[26] The numerical value of  $\tilde{c}_3^O$  and  $\tilde{h}$  can be obtained from the values of the oceanic tidal angular momentum (OTAM). They are given in terms of the OTAM height  $\tilde{H}^h$  and current  $\tilde{H}^c$  terms which are defined as:

$$\begin{cases} \tilde{H}^h = \tilde{c}_3^M \Omega_0 = \frac{\tau}{\tau - \chi} \tilde{c}_3^O \Omega_0 \\ \tilde{H}^c = \tilde{h}. \end{cases} \quad (15)$$

where we used the fact that, from equations (9) and (10),  $\tilde{c}_3^M = \frac{\tau}{\tau - \chi} \tilde{c}_3^O$ . We use the OTAM numerical value from *Chao et al.* [1996] given for the  $Q_1$ ,  $O_1$ ,  $P_1$  and  $K_1$  diurnal tides.

[27] Numerical values of OTAM at other diurnal frequencies are extrapolated from the values at  $Q_1$ ,  $O_1$ ,  $P_1$  and  $K_1$  with an empirical procedure developed by *Wahr and Sasao* [1981]. This procedure relies on the assumption that the OTAM at a given frequency  $\sigma$  can be obtained from the value at the frequency  $\sigma_0$  from [*Wahr and Sasao*, 1981, equation (4.8)]:

$$\tilde{c}_3^O(\sigma) = R(\sigma, \sigma_0) D(\sigma, \sigma_0) \frac{\tilde{\phi}(\sigma)}{\tilde{\phi}(\sigma_0)} \tilde{c}_3^O(\sigma_0). \quad (16)$$

This expression has been obtained by noting that the tidal sea level height function used by these authors is proportional to  $\tilde{c}_3^O$ .

[28] The  $R(\sigma, \sigma_0)$  factor in equation (16) is a real-valued function which is resonant at the FCN-frequency. Its expression, given by equation (4.5) of *Wahr and Sasao* [1981], depends on the frequency-dependent body and load Love numbers. We use the numerical values of the body Love numbers from *Wahr* [1981] and the load Love number from *Wahr and Sasao* [1981]. Those expressions of the Love numbers depend on the FCN-frequency that we fix here to  $-1.00232$  cpsd, which corresponds to a period of 430 d in space, the value obtained in MHB.

[29] The  $D(\sigma, \sigma_0)$  factor in equation (16) describes the effects due to all the dynamical processes taking place in the ocean. It is assumed to be a complex-valued function which varies smoothly with  $\sigma$  in the diurnal band. We assume this function to be linear:

$$D^{h,c}(\sigma, \sigma_0) = d_0^{h,c} + d_1^{h,c}(\sigma - \sigma_0), \quad (17)$$

where the superscripts  $h$  and  $c$  hold for the height and current terms respectively. The complex constants  $d_0^{h,c}$  and  $d_1^{h,c}$  are those which give the best fit of equation (16) to the data of *Chao et al.* [1996]. For  $\sigma_0 = \sigma_{O1}$ , we obtained the values  $d_0^h = 1.0255 - 0.0165i$ ,  $d_1^h = 3.5476 + 0.8212i$ ,  $d_0^c = 1.0246 - 0.0833i$  and  $d_1^c = 0.2608 + 3.3782i$ .

[30] We note here that, as mentioned above, we use in the expression of  $R(\sigma, \sigma_0)$  a fixed frequency of the FCN resonance from MHB. This may seem to be inconsistent because this resonance frequency depends strongly on the dynamical ellipticity of the fluid core, one of the parameters we have to adjust to the observations. This apparent inconsistency can be resolved by noting that the value of the core ellipticity can only have a significant influence on  $R$  at frequencies close to the FCN resonance. Because those frequencies are far from P1, O1, Q1 and K1 waves, the error coming from the extrapolation method will be larger than that coming from a small variation in the FCN frequency, which is rather accurately determined. Moreover, the value of OTAM at the four waves does also have an uncertainty which is not given by the ocean tide models. From those considerations and by noting that, in the frequency band close to the FCN resonance, the tide generating potential has relatively small amplitudes, we consider that fixing the FCN resonance to a given value for the purpose of computing  $\tilde{c}_3^O(\sigma)$  from equation (16) is a reasonable approximation.

### 2.3. Unmodeled Effects

[31] In the nutation model presented herein, some effects are not explicitly included: the geodesic nutation, the contributions from nonlinear terms, the atmospheric effects, and the excitation of the Free Core Nutation (FCN) mode. The way those effects are however taken into account is described here.

[32] The contribution of the geodesic nutation has been estimated by MHB and their numerical values can be found in Table 7 of their paper. As was done in MHB, we subtract those values from the data, prior to the inversion. The contributions from nonlinear terms, computed by *Lambert and Mathews* [2006], are also subtracted from the data before the inversion.

[33] The atmospheric effects on nutation are mainly due to thermal tides generated by the heating of the atmosphere by the Sun, which affects primarily the prograde annual term of nutation. Atmospheric tides excited by the external tidal potential have a smaller effect. The atmospheric contribution to the prograde annual term has been computed by *Bizouard et al.* [1998]. This estimate is however very dependent on the considered data set [*Yseboodt et al.*, 2002]. In this paper, following MHB, the atmospheric contribution to the prograde annual term is modeled by an additional unknown parameter of the nutation model. Note that this parameter also contains other effects giving rise to a

correction on the prograde annual term, such as the solar heating of the VLBI antennas [*Herring et al.*, 1991].

[34] In addition to the forced nutations described by equation (14), a free oscillation due to the excitation of the FCN mode by the geophysical fluids is observable in the VLBI data. Atmospheric pressure variations in the diurnal band are considered as an important cause of the excitation of the FCN [e.g., *Sasao and Wahr*, 1981]. However, *Lambert* [2006] shows that those atmospheric contribution to the FCN only accounts for roughly one half of the amplitude of the FCN observed in the VLBI data. Moreover, this author shows that, at the present level of accuracy of the atmospheric data, the time variability of the atmospheric forcing does not explain the time variability of the observed FCN amplitude. The contributions from other geophysical fluids, like the oceans, are still less known. For those reasons, in our paper, the oscillation is dealt with empirically, without any physical forcing, as a periodic term whose amplitude is variable in time. This time-variable amplitude is estimated in section 6.2 and then is subtracted from the data prior to the estimation of the nutation model parameters.

### 2.4. Earth Interior Parameters to be Estimated From Nutation Data

[35] The nutation model depends on several Earth internal structure parameters denoted by  $\mathbf{g}$  in the previous equations. Among them, some have a large influence on the nutational response of the Earth. They have been put forward by MHB and are listed in the part ‘‘Geophysical Parameters’’ of Table 1. They are the dynamical ellipticities of the whole Earth and fluid core, the complex compliances describing the deformation of the Earth and fluid core under the action of the tidal potential, namely  $\kappa$  and  $\gamma$  from equation (2) and the complex coupling constants  $K^{CMB}$  and  $K^{ICB}$ . Because of their large influence on nutation, their numerical values are estimated from the nutation observations.

[36] The other Earth interior parameters (e.g., the dynamical ellipticity of the solid inner core, the compliances for the deformability of the Earth and fluid core due to the centrifugal potentials of the outer and inner cores, the compliances for the deformations of the inner core, . . .), because of their rather weak influence on nutation, are fixed to the values computed by *Mathews et al.* [1991b] from the PREM model of *Dziewonski and Anderson* [1981].

[37] Concerning the estimation of the compliances  $\kappa$  and  $\gamma$  from the observations, note that, in this paper, we estimate the real and imaginary parts of the compliances from the observations. In MHB, the compliances are expressed as the sum of the compliance for a hypothetic purely elastic Earth and a complex correction due to mantle anelasticity. The complex correction is computed independently, from the integration of the deformation equations, using a model of the anelasticity such as the one of *Wahr and Bergen* [1986]. This correction is then fixed in the nutation model and the real compliance for the hypothetic elastic Earth is fit to the nutation observations. The direct estimation of the complex compliances performed in this paper allows to free ourselves from a priori anelasticity modeling and get directly the compliances from nutation data.

[38] As the inertial coupling, due to the ellipsoidal shape of the fluid core, cannot be separated from an additional

**Table 1.** Parameters to be Adjusted to the Nutation Observations<sup>a</sup>

Symbol	Definition	PREM
<i>Geophysical Parameters</i>		
$e$	dynamical ellipticity of the whole Earth	$3.247 \cdot 10^{-3}$
$e^f$	dynamical ellipticity of the fluid core	$2.548 \cdot 10^{-3}$
$\kappa$	complex compliance of the whole Earth	$1.039 \cdot 10^{-3}$
$\gamma$	complex compliance of the fluid core	$1.965 \cdot 10^{-3}$
$K^{CMB}$	complex coupling constant at the CMB	—
$K^{ICB}$	complex coupling constant at the ICB	—
<i>Atmospheric Contribution to the Prograde Annual Term</i>		
$a_{pa}$	complex correction to the amplitude of this term	
<i>Time Dependence Parameters</i>		
$d\Delta\epsilon/dt$	obliquity rate	
$c_\psi, c_\epsilon$	constant offsets	
<i>Probabilistic Modeling Parameter</i>		
$\sigma_M$	standard deviation of the Gaussian modeling uncertainty	

<sup>a</sup>For the geophysical parameters, the numerical values from PREM Earth model of *Dziewonski and Anderson* [1981] are listed.

coupling at the CMB due to another mechanism, the dynamical ellipticity  $e^f$ , related to the flattening of the fluid core, cannot be estimated independently from the real part of the coupling constant at the CMB. We therefore choose to estimate directly the sum  $e^f + \text{Re}(K^{CMB})$  from the observations. The physical interpretation of the estimated parameter requires a physical modeling of the coupling mechanism at the CMB, which allows to determine  $K^{CMB}$ .

[39] When estimating the complex coupling constant  $K^{CMB}$  and  $K^{ICB}$ , we do not assume (as was done by MHB) that the torques are of electromagnetic origin. We consider that the coupling constants contain contributions from several interactions between the different regions of the Earth: electromagnetic, topographic and viscous couplings. In this paper, we do not try to separate those contributions.

[40] The atmospheric effects on the prograde annual term is handled in MHB as follow: they observe that a residual is persistently found on the prograde annual nutation so that they decide to remove this residual from the data before the final fit of the nutation model. In this paper, we consider a correction term  $a_{pa}$  on the prograde annual nutation as an additional parameter which is estimated simultaneously with the other parameters.

[41] We notice here that in MHB, beside the geophysical parameters, there are several empirical parameters which are adjusted to the observations prior to the final fit. Those parameters are (1) a scaling of the mantle anelasticity contribution by a factor 1.09 (see MHB, section 2.3), in order to account for the imperfection of the frequency-to-the-power-alpha law used for anelasticity and (2) a scaling of the ocean tide current contribution by the large factor 0.7 (see MHB, section 2.5 [50]) in order to account for imperfections in the ocean current computation due to the fact that large contributions to this quantity come from small areas where the ocean is very deep.

[42] In this paper, we choose to not estimate scaling factors on the physical effects (ocean tide and anelasticity), unlike what was done in MHB, in order to stay as close as possible to the physics. They are introduced in MHB in order to cope for imperfection in modeling of those effects, but we prefer to use the present best solution for these effects. Instead of those scaling factors, as presented in

section 5.3, we include modeling uncertainties which also allow to take into account imperfections of the model.

[43] However, in order to compare our results with that of MHB, in addition to our main estimation without the scaling factors, we also perform an estimation with the 0.7 factor on the ocean tide currents and the results of this estimation are reported in section 7.

[44] In addition, in *Herring et al.* [2002], the a priori standard deviations on the nutation data series are increased by means of a procedure relying on a Kalman filtering technique [*Herring et al.*, 1990]. This correction implies also additional parameters which are calculated prior to the final fit of the geophysical parameters. We do not perform such an increase of the standard deviations, however, as we will show in section 5.3, the modeling uncertainties included in our inversion method can be interpreted equivalently as an additive correction to the standard deviations of the data. The main difference is that the parameter associated with the modeling uncertainty is estimated jointly with the geophysical parameters.

### 3. Time Domain Nutation Model

[45] In order to estimate the geophysical parameters from the time domain data, we express the nutation model as a function of time rather than of frequency as presented in equation (14). This conversion can be achieved quite simply by noting that, to a very good degree of approximation, the gravitational torque can be written as:

$$\hat{\phi}(t) = \sum_{l=1}^{3026} \tilde{\phi}(\sigma_l) e^{j \arg(\sigma_l, t)}, \quad (18)$$

where 3026 is the number of terms in the RDAN97 rigid nutation series and  $\arg(\sigma_l, t) = \sum_{i=1}^{10} N_i(\sigma_l) F_i(t)$ . The  $\{F_i(t)\}_{i=1, \dots, 10}$  are the fundamental arguments of nutation (namely the five Delaunay variables and the mean longitude of Venus, Mars, Jupiter, Saturn and Mercury) whose numerical expressions are given by *Simon et al.* [1994]. Each term of the torque, or equivalently, each term of the rigid Earth nutation is identified by its value of the multipliers of the fundamental arguments  $\{N_i(\sigma_l)\}_{i=1, \dots, 10}$ . The fundamental arguments are polynomial of the fourth order in time but the coefficients of terms larger than one are

so small that, for every practical purposes, they can be approximated by the first order polynomial in time:  $\arg(\sigma_l, t) \simeq \sigma_l \Omega_0 t + \alpha_l$ .

[46] Because the dynamical differential equations are linear, the nutation can be computed with equation (14) for each periodic term of the gravitational forcing of frequency  $\sigma$ . The total nutational motion in the time domain is thus obtained by summing all the contributions from each periodic term:

$$\hat{\eta}(\mathbf{g}, t) = \sum_{l=1}^{3026} \tilde{\eta}(\mathbf{g}, \sigma_l) e^{i \arg(\sigma_l, t)} \quad (19)$$

[47] In addition to the periodic nutation, the observations contain linear trends that are interpreted in terms of a secular drift in the precession and obliquity rates:

$$\hat{\eta}(\boldsymbol{\theta}, t) = \sum_{l=1}^{3026} \left( \tilde{\eta}(\mathbf{g}, \sigma_l) e^{i \arg(\sigma_l, t)} \right) + \left( P(\mathbf{g}) \sin(\epsilon_0) + i \frac{d\Delta\epsilon}{dt} \right) \cdot (t - t_0) + c_\psi \sin(\epsilon_0) + i c_\epsilon. \quad (20)$$

[48] In this equation,  $d\Delta\epsilon/dt$  is the obliquity rate and  $c_\psi$ ,  $c_\epsilon$  are constant offsets. Those three parameters will be estimated from the observations together with the geophysical parameters  $\mathbf{g}$  and are listed in Table 1. The vector  $\boldsymbol{\theta}$  in equation (20) represents all the parameters of the nutation model that will be adjusted to the observations except the last parameter of Table 1 which will be introduced in section 5.3.

[49] The correction to the precession rate,  $P$ , can be expressed in terms of the geophysical parameters and in particular in terms of the dynamical ellipticity  $e$ . Following MHB, we expand the precession rate by assuming that the precession rate for the nonrigid Earth is close to that of the rigid one:

$$P(\mathbf{g}) = P(H) = P_R(H_R) + \frac{dP_R}{dH_R} (H - H_R) + P_{NR}, \quad (21)$$

where  $P_R$  is the precession rate of the rigid Earth,  $H$ ,  $H_R$  are the precession constants of the nonrigid and rigid Earth respectively (the precession constant  $H$  is related to  $e$  by  $H = e/(1 + e)$ ) and  $P_{NR}$  represents the nonrigid contributions.

[50] The numerical values for some parameters in equation (21) are given in MHB:  $P_{NR} = -0.2015$  mas  $\text{a}^{-1}$  and  $dP_R/dH_R = 15397060$  mas  $\text{a}^{-1}$  but the authors do not precise which rigid Earth model they use for  $H_R$  and  $P_R(H_R)$ . In order to be consistent with the value of  $dP_R/dH_R$ , computed by Bretagnon, we used  $H_R$  and  $P_R(H_R)$  from the rigid Earth model of *Bretagnon et al.* [1998]:  $H_R = 0.0032737668$  and  $P_R(H_R) = 50384.566$  mas  $\text{a}^{-1}$ .

[51] The numerical value of  $t_0$  has been chosen such that the correlation between the slopes ( $P$  and  $d\Delta\epsilon/dt$ ) and the intercepts ( $c_\psi$  and  $c_\epsilon$ ) of the linear trend be minimal. For the simple case of fitting a straight line on data, it has been shown [e.g., *Gregory, 2005*] that the correlation between the slope and intercept is zero if the origin time is the weighted average of the time indices of the data:  $t_0 = \sum_i w_i t_i / \sum_i w_i$ , where  $w_i = \sigma_i^{-2}$ , the inverse of the squared standard

deviations on the data. Using the standard deviations on  $\Delta\psi$ , or equivalently on  $\Delta\epsilon$ , we get:  $t_0 = 2000.64$  year.

## 4. Nutation Data

[52] The nutation data used in this paper are obtained from the very long baseline interferometry (VLBI) technique and are provided by the international VLBI service (IVS). We use the data series “gsf2007b.eops” which is the most recent analysis of the Goddard Space Flight Center (GSFC). Those data range over the time period from 1982.7 to the middle of 2007. They are available at <http://ivscc.gsfc.nasa.gov/products-data/products.html>.

## 5. Bayesian Inversion Method

[53] In this paper, we use Bayesian inversion in order to get an estimation of the Earth interior parameters from the nutation observations. In the nutation model, the Earth interior parameters enter in the model in a highly nonlinear way. Because the Bayesian method does not make any linearization of the model with respect to its parameters, this method is particularly well suited to deal with that model. We present here the main features of the method.

### 5.1. Bayesian Approach

[54] Because random errors are always associated with measurements, data are only one particular realization of a random variable. The probability that, given a particular value of the parameters  $\boldsymbol{\theta} = \{\theta_1, \dots, \theta_n\}$ , the data vector  $\mathbf{d}$  is measured is expressed by the likelihood function  $L(\mathbf{d}|\boldsymbol{\theta})$ . Physical modeling determines the so-called forward problem,  $\mathbf{d} = M(\boldsymbol{\theta})$ , relating the parameters to the error-free data by a physical model  $M$ . Knowledge of the statistical properties of the measurement noise allows then to get the likelihood function, also called the forward probability density function (pdf). Rather than this forward probability, we are interested in knowing the probability  $p(\boldsymbol{\theta}|\mathbf{d})$  that the parameters have the value  $\boldsymbol{\theta}$ , given that the observations  $\mathbf{d}$  have been obtained. This pdf is called the posterior pdf.

[55] The method relies on Bayes’ theorem which allows to infer the posterior pdf from the knowledge of the forward pdf. It can be expressed as:

$$p(\boldsymbol{\theta}|\mathbf{d}) = c L(\mathbf{d}|\boldsymbol{\theta}) \cdot \pi(\boldsymbol{\theta}). \quad (22)$$

In this equation, the pdf  $\pi(\boldsymbol{\theta})$ , called the prior pdf, represents the knowledge of the parameters independent of the observations. The constant of proportionality  $c$  is obtained by normalization of the posterior pdf and is equal to:

$$c^{-1} = \int_{\text{all models}} L(\mathbf{d}|\boldsymbol{\theta}) \pi(\boldsymbol{\theta}) d\boldsymbol{\theta}, \quad (23)$$

where “all models” stands for all the values of the parameters  $\boldsymbol{\theta}$ .

[56] The output of the Bayesian inversion is the posterior pdf. From the posterior pdf, marginals can be computed for each parameter  $\theta_i$ ,  $i = 1, \dots, n$ :

$$p(\theta_i|\mathbf{d}) = \int p(\boldsymbol{\theta}|\mathbf{d}) d\theta_1 \dots d\theta_{i-1} d\theta_{i+1} \dots d\theta_n \quad (24)$$

If estimated values and associated error are needed, they can be obtained from the marginals by estimating the mean and variance:

$$\bar{\theta}_i = \int p(\theta_i | \mathbf{d}) \theta_i d\theta_i \quad (25)$$

$$\bar{\sigma}_{\theta_i}^2 = \int p(\theta_i | \mathbf{d}) (\theta_i - \bar{\theta}_i)^2 d\theta_i \quad (26)$$

Also the value of the parameter which maximizes the marginal pdf (maximum a posteriori, MAP, solution) can be used.

[57] With the assumption that the noise of the nutation observations is independent from one measurement to the other and is normally distributed, the posterior pdf for the parameters of the nutation model can be written:

$$p(\boldsymbol{\theta} | \{\Delta\psi_t^d, \Delta\epsilon_t^d\}) \propto \prod_{i=0}^N (\sigma_t^\epsilon \sigma_t^\psi \sin \epsilon_0)^{-1} \pi(\boldsymbol{\theta}) \times \exp \left[ - \sum_{i=0}^N \left\{ \frac{(\Delta\epsilon(\boldsymbol{\theta}, t_i) - \Delta\epsilon_t^d)^2}{2(\sigma_t^\epsilon)^2} + \frac{(\Delta\psi(\boldsymbol{\theta}, t_i) - \Delta\psi_t^d)^2}{2(\sigma_t^\psi)^2} \right\} \right] \quad (27)$$

where  $\Delta\psi_t^d$  and  $\Delta\epsilon_t^d$  are the nutation data, in longitude and obliquity, in time series, at the epochs  $t_i = \{t_0, \dots, t_N\}$  and  $\sigma_t^\epsilon$  and  $\sigma_t^\psi$  are the corresponding standard deviations. We note that, as mentioned in the Introduction, it is indeed the standard deviations in the time domain which are directly used for the estimation. This allows to take their time variations into account when estimating the geophysical parameters. In equation (27),  $\Delta\psi(\boldsymbol{\theta}, t_i)$  and  $\Delta\epsilon(\boldsymbol{\theta}, t_i)$  are the theoretical longitude and obliquity corresponding to the real (divided by  $\sin \epsilon_0$ ) and imaginary part of the complex nutation computed with equation (20), while  $\pi(\boldsymbol{\theta}) = \prod_{i=1}^n \pi(\theta_i)$  is the prior pdf for the parameters which will be discussed in section 5.4.

## 5.2. Stochastic Sampling

[58] In most cases, the posterior pdf and the estimates given by equations (25)–(26) cannot be computed neither analytically nor even numerically so that the posterior is sampled with a stochastic method. In this paper, we use the Metropolis-Hasting algorithm [Metropolis *et al.*, 1953; Hastings, 1970] which generates a Markov chain whose equilibrium distribution is the posterior pdf. This algorithm allows to obtain an empirical pdf which approximates the posterior pdf. From this empirical pdf, the mean and variance of the marginals defined by equations (25)–(26) can be approximated by replacing the integrals by finite sums.

## 5.3. Inclusion of Modeling Uncertainties

[59] In writing the posterior pdf in equation (27), we implicitly make the assumption that the theoretical model of nutation is “perfect” in the sense that it explains all the physical signal in the data. This assumption is always

implicitly made in the classical inversion methods like least squares fit and, in particular, in the estimation of MHB.

[60] However, this assumption of perfect model is quite unrealistic and, in this paper, we propose to take into account the possibility of having modeling uncertainties. This is motivated by several reasons: the Earth interior model is quite simple, the ocean tides contributions are computed from ocean models which assimilate some data (with unknown uncertainties), the atmospheric contributions to nutation are poorly known, etc.

[61] Because the modeling uncertainties cannot be quantified, we make the assumption that they follow a Gaussian distribution with an unknown standard deviation. We consider that the standard deviation of the Gaussian modeling uncertainty is constant with time and we denote it  $\sigma_M$ .

[62] It has been shown [e.g., Gregory, 2005, chapter 4; Tarantola, 2005, chapter 1] that, in the case of Gaussian modeling uncertainties, the posterior probability on the parameters can be written as:

$$p(\boldsymbol{\theta}, \sigma_M | \{\Delta\psi_t^d, \Delta\epsilon_t^d\}) \propto \pi(\sigma_M) \pi(\boldsymbol{\theta}) \times \prod_{i=0}^N \left\{ (\sigma_t^\epsilon)^2 + \sigma_M^2 \right\}^{-1/2} \left\{ (\sigma_t^\psi \sin \epsilon_0)^2 + \sigma_M^2 \right\}^{-1/2} \times \exp \left[ - \sum_{i=0}^N \left\{ \frac{1}{2} \frac{(\Delta\epsilon(\boldsymbol{\theta}, t_i) - \Delta\epsilon_t^d)^2}{(\sigma_t^\epsilon)^2 + \sigma_M^2} + \frac{1}{2} \frac{(\Delta\psi(\boldsymbol{\theta}, t_i) - \Delta\psi_t^d)^2 (\sin \epsilon_0)^2}{(\sigma_t^\psi \sin \epsilon_0)^2 + \sigma_M^2} \right\} \right] \quad (28)$$

where we have made the hypotheses that the uncertainties are independent and normally distributed for the modeling uncertainties as well as the observations. Note that we assume that the modeling uncertainties for the longitude and obliquity components of the nutation motion have the same standard deviation.

[63] As the standard deviation of the Gaussian modeling uncertainty is unknown (e.g., the ocean tide contributions are given without any estimation of their error), we estimate this parameter from the data together with the other parameters of the model. In equation (28),  $\pi(\sigma_M)$  represents the prior probability for this parameter.

[64] Besides the fact that the nutation model is not perfect, there is another argument in favor of the inclusion of modeling uncertainties. In equation (28), the parameter  $\sigma_M$ , introduced as the error coming from the imperfect modeling, is indistinguishable from an additive Gaussian error in the observations. This implies that the inversion with modeling uncertainties also takes into account the possibility of having too small standard deviations on the data and estimates an additive correction together with the other parameters. This is adequate for VLBI nutation data because their standard deviation are suspected to be underestimated. This is for the same reason that Herring *et al.* [2002], as mentioned before, compute, before the fit of the parameters, corrections to the standard deviations of the nutation data. Our correction of the standard deviations is more consistent because it is contained in the parameter  $\sigma_M$

**Table 2.** Bounds on the Prior pdf's for the Parameters to be Estimated From the Data

Parameter	Lower Bound	Upper Bound
$e$	$3.2 \times 10^{-3}$	$3.3 \times 10^{-3}$
$e^f + \text{Re}(K^{CMB})$	$2 \times 10^{-3}$	$3 \times 10^{-3}$
$\text{Re}(\kappa)$	$5 \times 10^{-4}$	$5 \times 10^{-3}$
$\text{Im}(\kappa)$	$-10^{-3}$	$10^{-3}$
$\text{Re}(\gamma)$	$1.5 \times 10^{-3}$	$2.5 \times 10^{-3}$
$\text{Im}(\gamma)$	$-10^{-3}$	$10^{-3}$
$\text{Im}(K^{CMB})$	$-10^{-2}$	$-10^{-7}$
$\text{Re}(K^{ICB})$	$10^{-7}$	$10^{-2}$
$\text{Im}(K^{ICB})$	$-10^{-2}$	$-10^{-7}$
$\text{Re}(a_{pa})^b$	-1	1
$\text{Im}(a_{pa})^b$	-1	1
$d\Delta\epsilon/dt^a$	-1	1
$c_{\psi}^b$	-100	100
$c_{\epsilon}^b$	-100	100
$\sigma_M^b$	$10^{-7}$	10

<sup>a</sup>Units: mas a<sup>-1</sup>.<sup>b</sup>Units: mas.

which is estimated simultaneously with the geophysical parameters.

#### 5.4. Choice of the Prior Distributions

[65] The prior distributions for the parameters  $e$ ,  $e^f + \text{Re}(K^{CMB})$ ,  $\text{Re}(\kappa)$ ,  $\text{Im}(\kappa)$ ,  $\text{Re}(\gamma)$ ,  $\text{Im}(\gamma)$ ,  $\text{Re}(a_{pa})$ ,  $\text{Im}(a_{pa})$ ,  $d\Delta\epsilon/dt$ ,  $c_{\psi}$ , and  $c_{\epsilon}$  are chosen to be uniform between reasonable bounds. The bounds for each parameter are listed in Table 2. The reasonable range of values for the dynamical ellipticities and the compliances are known from the computation of these quantities with different Earth models [e.g., Mathews *et al.*, 1991b]. The values of  $\text{Re}(a_{pa})$  and  $\text{Im}(a_{pa})$  have been computed by Bizouard *et al.* [1998] and that of  $d\Delta\epsilon/dt$  has been estimated from different data analysis what allows to put lower and upper bounds on those parameter.

[66] The parameter  $\sigma_M$  which represents a standard deviation must be positive to make sense so that its prior distribution is chosen to be a Jeffrey's distribution [e.g., Gregory, 2005] defined in general, for  $x \neq 0$ , by:

$$p(x) = \begin{cases} \frac{k}{x} & \text{if } x_{\min} < x < x_{\max} \\ 0 & \text{elsewhere} \end{cases} \quad (29)$$

with  $1/k = \text{Log}(x_{\max}/x_{\min})$ . In order to impose the positiveness of the parameter  $\sigma_M$ , we choose positive bounds  $x_{\min}$ ,  $x_{\max}$  with  $x_{\min}$  close to zero.

[67] The sign of the coupling constants have been computed by Buffett *et al.* [2002] and must be such that  $\text{Re}(K^{CMB}) > 0$ ,  $\text{Re}(K^{ICB}) > 0$ ,  $\text{Im}(K^{CMB}) < 0$  and  $\text{Im}(K^{ICB}) < 0$ . We use Jeffrey's prior for those parameters too, with positive or negative bounds listed in Table 2.

## 6. Inversion of the Time Domain Data

### 6.1. Simulations

[68] In order to test whether the nutation model and the Bayesian inversion described previously allow to estimate reliably the geophysical parameters, we made some simu-

lations. We created synthetic data from the time domain nutation model of equation (20), with the parameters fixed to some reasonable numerical values, to which we add Gaussian observational errors and a Gaussian modeling error. The observational errors are simulated using the time dependent standard deviations from the GSFC VLBI data while the constant standard deviation of the modeling error is equal to that we obtained by inverting the true data.

[69] We performed the Bayesian inversion of those synthetic data and compare the estimates obtained for each parameter with their true value. The result is that, for each parameter, the true value lies in the  $2\sigma$  domain of the estimated value.

### 6.2. Estimation of the Amplitude of the FCN Mode

[70] In order to estimate the time-dependent amplitude of the free FCN mode, we perform a first inversion of the VLBI data with the method described above and with the nutation model without any modeling of the free mode. This inversion provides a joint posterior probability for the parameters, conditioned on the data, from which the residuals of the model can be computed with the following estimator:

$$\bar{\mathbf{r}} = \int (\mathbf{d} - M(\boldsymbol{\theta}))p(\boldsymbol{\theta}|\mathbf{d})d\boldsymbol{\theta} \quad (30)$$

where  $\mathbf{d}$  is the data vector,  $p(\boldsymbol{\theta}|\mathbf{d})$  is the joint posterior on the parameters  $\boldsymbol{\theta}$ , and  $M$  is the physical model. By using the empirical joint posterior, the integral of equation (30) is replaced by a finite sum.

[71] We estimate the time-dependent amplitude  $a_f(t)$  of the free mode by fitting to those residuals the following expression:

$$\eta_f(t) = -ia_f(t)e^{i2\pi F_f(t-t_{2000})} \quad (31)$$

where  $F_f$  is the frequency of the FCN mode which is determined from the estimated geophysical parameters using the first relation of equation (33). In equation (31),  $t_{2000}$  is the time on 1 January 2000 which is taken as reference for the phase. This fit is performed with a weighted least squares method, as equation (31) is linear in the parameter  $a_f$  to be estimated. The amplitude is estimated once per year from a four years-interval centered on that time. The real and imaginary part of  $a_f$  obtained by this procedure are presented on the Figure 1.

[72] Figure 1 supports the well-known fact [e.g., Herring *et al.*, 2002] that the amplitude of the free FCN mode changes significantly during the period where nutation data are available. On the interval from 1984 to 2000, our results are similar to that obtained by Herring *et al.* [2002]. The additional time span from 2000 to 2005 reveals that the free oscillation, which was nearly vanishing around the year 2000, is again increasing in amplitude. We compared our results to that of the IERS Conventions (updates to Chapter 5, 2007), available at <ftp://tai.bipm.org/iers/convupdt/chapter5/icc5.pdf>. We showed that our results are a bit different for the period from 1984 to 1989 but are very similar for the period after 1989.

[73] From this estimated time-dependent amplitude, the oscillation of the free mode is reconstructed and removed

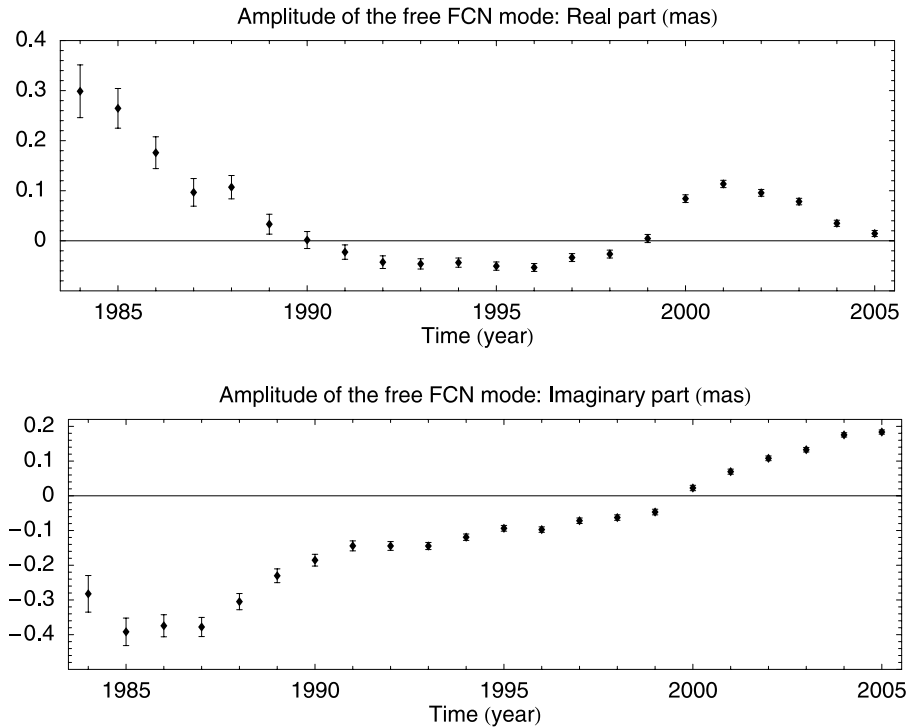


**Figure 1.** Time-dependent amplitude of the free FCN mode. Error bars correspond to three standard deviations.

from the data before the final inversion presented in the section 6.3. The parameters estimated from the final inversion are compatible with those of the first estimation (performed without any modeling of the free mode), in the sense that, for each parameter, the estimates of the second inversion are within the one-sigma interval around the estimates of the first inversion. Only the estimate of the parameter  $\sigma_M$ , characterizing the modeling error, is smaller in the second estimation what makes sense because, in the second inversion, the FCN free mode has been taken into account. Finally, the estimated errors on the parameters (computed from the standard deviations of the corresponding marginals) are reduced in the second inversion by a factor between 5 and 20%.

### 6.3. Results From the Inversion of the VLBI Data

[74] We present now the results of the inversion of the VLBI nutation data from the GSFC, performed with the nutation model and the Bayesian inversion method described in the previous sections.

[75] The stochastic sampling of equation (28) provides an empirical posterior probability, from which we can get the marginal probabilities for each parameter. The marginal probabilities are represented by the histograms in the Figures 2 and 3.

[76] From the posterior density we estimate for each parameter the mean, the standard deviation, and the 99.7% confidence interval. As the confidence intervals are almost symmetric about the estimated mean, and the individual half widths of the intervals virtually 3 sigma's wide, we only report the mean and the 3 sigma wide uncertainty range in Table 3.

[77] The third column of Table 3 gives the numerical values from MHB. Because there are some differences between the parameters chosen to be adjusted in MHB and in this paper, some of their numerical results are adapted in order to be comparable. In particular, we add the numerical values of the  $\Delta\kappa^{AE}$  and  $\Delta\gamma^{AE}$  (anelasticity contribution to the compliances) introduced by MHB to their values of the elastic compliances in order to get the complete complex  $\kappa$  and  $\gamma$ , used in this paper. The value of  $\Delta\kappa^{AE}$  is given in Appendix D of MHB:  $\Delta\kappa^{AE} = (1.258 + 0.529i) 10^{-5}$ , without indication on the error, whereas their value of  $\Delta\gamma^{AE}$  is not given. Moreover, because the parameter  $e^f$  cannot be separated from  $\text{Re}(K_{CMB})$ , we add the value  $\text{Re}(K_{CMB}) = 0.5 (1.95 + 2.54) 10^{-5} = 2.245 10^{-5}$ , assumed in MHB (section 4.1), to their value of the estimated parameter  $e^f$ .

[78] In order to compare our numerical results with those obtained by MHB, the dashed vertical lines on Figures 2 and 3 represents the  $3\sigma$ -range of values obtained by MHB.

[79] The additional parameter, introduced in section 5.3, has been estimated to be  $\sigma_M = 0.219 \pm 0.008$  mas (corresponding to the mean and 3 standard deviations of the empirical marginal probability). In order to get an idea of the relative magnitude of the modeling and the observational uncertainties, note that the mean value of the standard deviation of the data, on the total period from 1982.7 to 2007.5, is of about 0.21 mas. The modeling uncertainty is thus of the same order of magnitude as the observational uncertainties. Note that the parameter  $\sigma_M$  does not only contain the modeling uncertainties but also a constant correction to the error on the data.

[80] Finally, we compute the residuals of the model, with the estimator given in equation (30). The magnitude of the

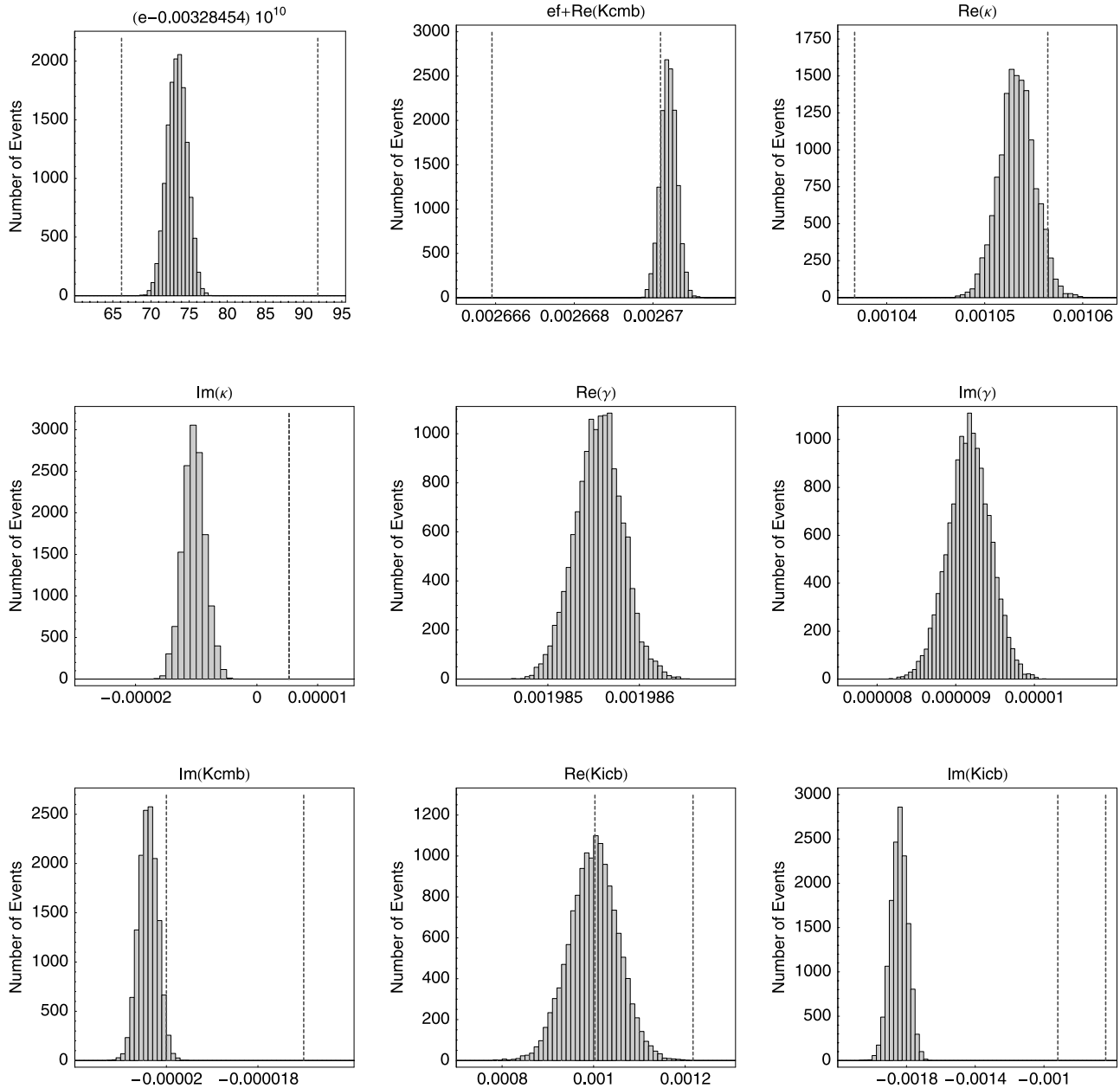


**Figure 2.** Empirical marginal posterior distributions for the geophysical parameters, obtained from the Bayesian inversion of the nutation data. For the parameters for which those values are available, the dashed vertical lines represent the  $3\sigma$ -range of values obtained by *Mathews et al.* [2002]. For the parameter  $\text{Im}(\kappa)$  the standard deviation of the estimation made by MHB is not known so that the dashed line represents their estimated value and there is no range of values.

residuals can be estimated by computing their weighted root mean squares (WRMS) defined by:

$$\text{WRMS}(\mathbf{r}, \boldsymbol{\sigma}) = \sqrt{\sum_i w_i r_i^2}, \quad \text{with } w_i = \frac{1/\sigma_i^2}{\sum_j 1/\sigma_j^2}, \quad (32)$$

where  $\mathbf{r} = \{r_i\}_{i=1, \dots, N}$  are the residuals and  $\boldsymbol{\sigma} = \{\sigma_i\}_{i=1, \dots, N}$  are the corresponding standard deviations. We get 0.257 mas and 0.153 mas for the  $\Delta\psi \sin(\epsilon_0)$  and  $\Delta\epsilon$  components respectively. Note that we also computed residuals as the difference between the data and the model with the value of

the parameters given in Table 3, and it gives the same WRMS. Using MHB nutation model with their estimation of the geophysical parameters, *Herring et al.* [2002] obtained the following WRMS of the residuals: 0.188 mas and 0.194 mas for the  $\Delta\psi \sin(\epsilon_0)$  and  $\Delta\epsilon$  components respectively.

## 7. Discussion of the Results

[81] In the previous section, a new estimation for the geophysical parameters is presented. In this section, we compare our results to those obtained by MHB.

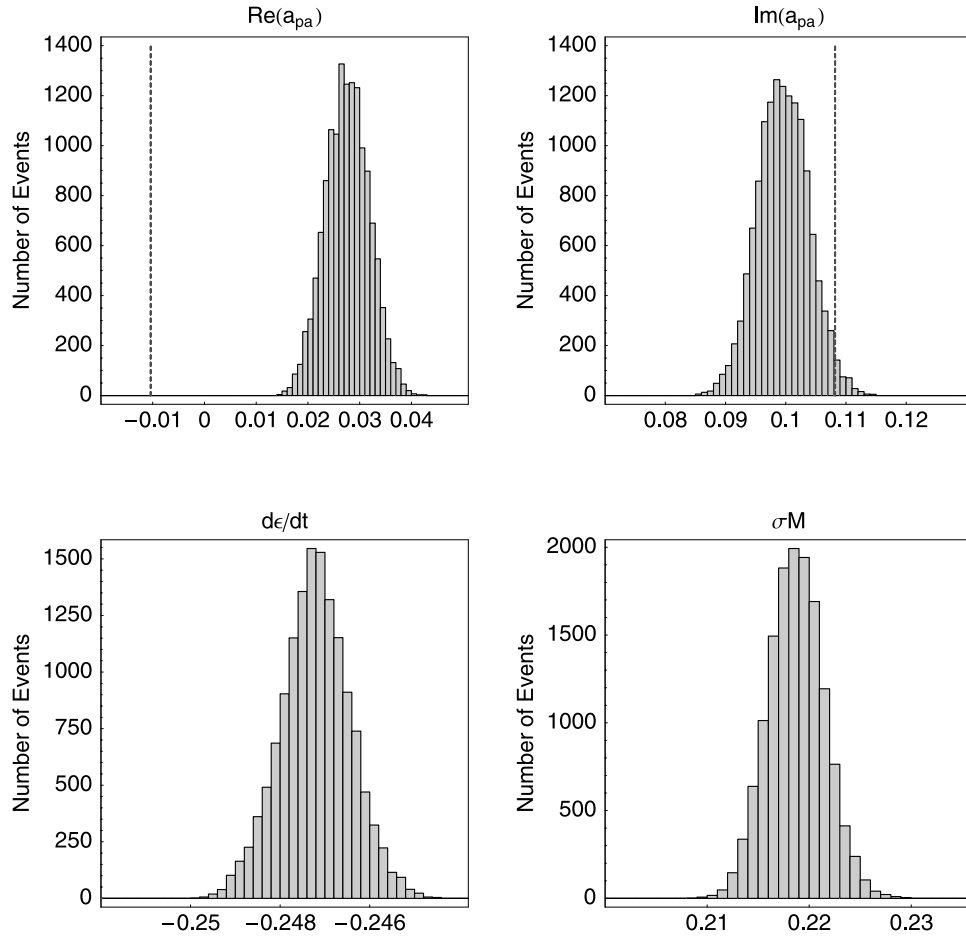


**Figure 3.** Empirical marginal posterior distributions for the correction to the amplitude of the prograde annual term, for the obliquity rate and for the standard deviation of the Gaussian modeling uncertainty, obtained from the Bayesian inversion of the nutation data.

### 7.1. Estimated Errors

[82] We begin the discussion by a comparison between the estimated errors in this paper and in MHB. For most parameters, our estimated errors are smaller by a factor from 1.7 to 3.7. This is due to three main reasons: (1) the different inversion strategy, (2) the different a priori standard error on the data: the standard error on the data used by MHB were increased [Herring *et al.*, 2002] prior to the estimation of the geophysical parameters, and (3) the additional 7 years of data.

[83] In order to estimate the influence of the additional data on the estimated errors on the parameters, we performed the same inversion with the data truncated in November 1999 as it was the case at the time MHB was published. The result is that the estimated errors on the parameters are larger than those obtained from our inversion with all the data, but still smaller than those of MHB, except for the real and imaginary part of  $K^{ICB}$  for which our estimation on the truncated data set gives very larger errors than MHB. Note however that the truncated data set used here is not the same as that used by MHB because the data sets have been entirely reprocessed since that time.

[84] The effect of the increased standard deviation of the data on the parameters error is more difficult to estimate because the data whose standard deviation were increased

by Herring *et al.* [2002] are frequency domain data and thus we cannot perform exactly the same modification of the

**Table 3.** Numerical Values of the Earth Interior Parameters and Comparison With the Values of Mathews *et al.* [2002]<sup>a</sup>

Parameter	This Paper	MHB
$e$	$0.0032845473 \pm 4$	$0.0032845479 \pm 13$
$\mathcal{J} + \text{Re}(K^{CMB})$	$0.0026704 \pm 6$	$0.0026680 \pm 21$
$\text{Re}(\kappa)$	$0.0010533 \pm 55$	$0.0010466 \pm 99$
$\text{Im}(\kappa)$	$-0.0000103 \pm 54$	$0.00000529$
$\text{Re}(\gamma)$	$0.00198555 \pm 78$	...
$\text{Im}(\gamma)$	$0.00000917 \pm 81$	...
$\text{Im}(K^{CMB})$	$-0.0000204 \pm 6$	$-0.0000185 \pm 15$
$\text{Re}(K^{ICB})$	$0.00100 \pm 16$	$0.00111 \pm 11$
$\text{Im}(K^{ICB})$	$-0.00184 \pm 15$	$-0.00078 \pm 14$
$\text{Re}(a_{pa})^c$	$0.028 \pm 13$	$-0.010$
$\text{Im}(a_{pa})^c$	$0.100 \pm 13$	$0.108$
$d\Delta\epsilon/dt^b$	$-0.2472 \pm 23$	...
$c_\epsilon^c$	$-7.087 \pm 15$	...
$c_\psi^c$	$-41.593 \pm 38$	...
$\sigma_M^c$	$0.2187 \pm 82$	...

<sup>a</sup>The second column gives the values for the inversion performed in this paper. The errors are on the last written digits and correspond to  $3\sigma$ . Numerical values obtained by Mathews *et al.* [2002] are listed in column three.

<sup>b</sup>Units:  $\text{mas a}^{-1}$ .

<sup>c</sup>Units: mas.

standard deviation in order to quantify the effect on the parameters error. However, we made the test of arbitrarily increasing the a priori standard deviation on the time domain data and we verify that it indeed increases the estimated error on the parameters.

[85] Whereas most of the parameters have smaller estimated error in this computation than in MHB, the parameters related to the coupling at the ICB,  $\text{Re}(K^{ICB})$  and  $\text{Im}(K^{ICB})$ , have similar or even larger estimated errors than theirs. This seems reasonable because those parameters are the lesser constrained by the nutation observations so that larger errors on these parameters could be more realistic.

## 7.2. Dynamical Ellipticities

[86] The estimation of the dynamical ellipticity  $e$  is in complete agreement with that of MHB. The estimated error on the parameter is 3 times smaller in this paper than in their one. However, because this parameter is mainly determined by the precession rate rather than by nutation, its numerical value is strongly dependent on the value used for the constants  $H_R$  and  $P_R(H_R)$  introduced in equation (21). Note that the numerical values used by MHB are not given in their paper. In order to free ourselves from the numerical values of those constants, we compare directly the precession rate induced by the estimated dynamical ellipticity. From our value of  $e$ , using equation (21), the precession rate (from which we subtract the IAU value:  $P_{IAU} = 50387.784 \text{ mas a}^{-1}$ ) is equal to  $P(e) - P_{IAU} = -2.994 \pm 0.006 \text{ mas a}^{-1}$  ( $3\sigma$  error) while MHB obtained  $P(e) - P_{IAU} = -2.997 \pm 0.020 \text{ mas a}^{-1}$  ( $3\sigma$  error). Our result for the correction to the precession rate induced by the dynamical ellipticity is thus also in agreement with MHB.

[87] However, we think that the agreement of our estimation of the dynamical ellipticity and precession rate with that of MHB is quite fortuitous because, depending on the length of the data time series, the estimated value is different. To illustrate this fact, we have estimated the dynamical ellipticity on data between 1979 and 2006, with the data set “gsf2005a.eops”, and we get the result:  $e = 0.0032845450 \pm 5$  which is not in agreement with MHB any more. This instability of the parameter  $e$  is due to the fact that the linear rate of the data (which gives the precession rate and thus constrains the dynamical ellipticity) is highly correlated to the main nutation term of frequency 18.6 year which is badly determined from the data because only 28 years of data are available, the first years of which being of low quality.

[88] Our estimation of the dynamical ellipticity of the fluid core  $e^f + \text{Re}(K^{CMB})$  is close to the upper limit of the  $3\sigma$  range of values determined by MHB, with an error 3.5 times smaller.

## 7.3. Compliances

[89] The compliances  $\kappa$  and  $\gamma$  are estimated in a different way in this paper than in MHB. As explained before, in MHB, the compliances are computed, independently of the nutation model, from a model of the anelasticity, while in this paper they are estimated from the data.

[90] Our estimation for the real part of  $\kappa$  is compatible with that of MHB with a slightly smaller error. Our estimation of  $\text{Im}(\kappa)$  is completely different from that of

MHB: our value is negative while MHB find a positive value (without indication of the error). This difference can be explained by the fact that, the value of MHB, because it has been computed theoretically from anelasticity models, represents purely the imaginary part of the compliance due to anelasticity. On the other hand, our value being estimated from the nutation data, it is contaminated by the mismodeling of the ocean tides effects, which give also rise to imaginary contributions to the compliances. The fact that our estimated value is negative (which is not physically meaningful, as the deformational response of the Earth must lag behind the forcing, see MHB Appendix C) reflects the imperfection in the ocean tides modeling. MHB also deduced from their computations that the ocean tide contributions must be somewhat erroneous and decided to scale the current oceanic term by a 0.7 factor. We have performed the test of doing the same inversion with this 0.7 factor applied to the ocean tide current contribution and the result is that all the parameters remains unchanged except two of them whose values become:  $\text{Re}(\kappa) = 0.0010415 \pm 66$  and  $\text{Im}(\kappa) = 0.0000093 \pm 62$  (where the errors are  $3\sigma$  and refer to the two last digits). This estimation for  $\text{Im}(\kappa)$  is in agreement with that of MHB.

[91] Note that we cannot interpret our result for  $\text{Im}(\kappa)$  in terms of the quality factor of the Chandler wobble because the imaginary part of the compliances, arising from the anelasticity contribution, is frequency dependent and the Chandler wobble is not in the frequency band of the nutation.

## 7.4. Coupling Constants

[92] Concerning the complex coupling constants at the CMB and ICB, the imaginary part of  $K^{CMB}$  is estimated slightly larger (in absolute value) in this paper than in MHB with a 2.5 times smaller error. The parameter  $\text{Re}(K^{ICB})$  is in agreement with MHB and our estimation of the error is larger than their one. The imaginary part of  $K^{ICB}$  is the parameter which is the most different between the two estimations: our estimation is more than two times larger (in absolute value) than MHB. The consequences of the new estimations for the coupling constants on the frequencies and quality factors of the RFCN and PFCN free modes are presented in section 7.7.

## 7.5. Correction to the Prograde Annual Term

[93] Our estimation of the corrective term on the prograde annual term is of the same order of magnitude as that of MHB. The imaginary part is compatible, as MHB value lies in the  $3\sigma$  interval of our estimation. The value computed by *Bizouard et al.* [1998] from the atmospheric angular momentum time series of the NCEP/NCAR reanalysis project is  $9.3 + i76.0 \mu\text{as}$ . *Yseboodt et al.* [2002] have shown that, depending on the atmospheric data set used, the value of the real part can go from  $-65.7 \mu\text{as}$  to  $8.4 \mu\text{as}$  and that for the imaginary part from  $9.9 \mu\text{as}$  to  $86.7 \mu\text{as}$ . Our estimation is larger in absolute value than these values, what suggests, as mentioned before, that other effects than the atmosphere contribute to the prograde annual term.

## 7.6. Additional Parameters

[94] Finally, four additional parameters are adjusted in this paper simultaneously with the geophysical parameters:

the obliquity rate  $d\Delta\epsilon/dt$ , the constant offsets  $c_{\psi}$  and  $c_{\epsilon}$  and the parameter  $\sigma_M$  introduced in section 5.3. However, we must note that, while their existence is not mentioned in MHB, those parameters (or parameters having a similar role) have been estimated by *Herring et al.* [2002], before the final fit of the geophysical parameters performed in MHB. In our paper, all the parameters included in the modeling are estimated altogether.

[95] The obliquity rate  $d\Delta\epsilon/dt$  and the constant offsets have been estimated by *Herring et al.* [2002] together with their estimation of the amplitudes of the 21 nutation frequencies. Their numerical result for the obliquity rate is  $d\Delta\epsilon/dt = -0.237 \text{ mas a}^{-1}$ , with standard deviation of  $0.012 \text{ mas a}^{-1}$ , while their estimated offsets are not given. Note that, for the obliquity rate, they multiplied their original value of the standard deviation, which was equal to  $0.003 \text{ mas a}^{-1}$ , by a factor of 4. The value estimated in this paper for the obliquity rate lies in the  $1\sigma$  range of the estimation by *Herring et al.* [2002]. However, our standard deviation is about three times smaller than their original one. Note that the numerical value obtained from theoretical computations by *Williams* [1994] is  $d\Delta\epsilon/dt = -0.244 \text{ mas a}^{-1}$ , which is quite close to our estimation.

[96] The parameter  $\sigma_M$  introduced in this paper incorporates both the modeling uncertainties and a constant correction to the standard deviation of the data. This parameter has thus partially the same goal as the parameters introduced by *Herring et al.* [2002] in order to correct the data errors. However, our parameter  $\sigma_M$  is introduced here in the theoretical frame of the Bayesian inversion for a probabilistic model, which is more consistent and allows an estimation of this parameter simultaneously with the geophysical ones.

### 7.7. Periods and Quality Factors of the Free Modes

[97] We end this section by describing the impact of this new parameter estimation on the periods and quality factors of the RFCN and PFCN resonances. The complex frequencies (in cycles per sidereal days) in the terrestrial frame are linked to the geophysical parameters by the approximated relations:

$$\begin{aligned} \sigma_{RFCN} &\simeq -1 - \frac{A}{A_m} \left( e^f - \beta + K^{CMB} + \frac{A_s}{A_f} K^{ICB} \right) \\ \sigma_{PFCN} &\simeq -1 + \alpha_2 e_s + \nu - K^{ICB} \end{aligned} \quad (33)$$

where  $A$ ,  $A_m$ ,  $A_f$  and  $A_s$  are the moment of inertia in the equatorial plane of the whole Earth, mantle, fluid core and solid inner core, respectively,  $e_s$  is the dynamical ellipticity of the inner core,  $\beta$  and  $\nu$  are the compliances defined by equation (2), and  $\alpha_2$  is an Earth parameter defined in *Mathews et al.* [1991a]. The numerical values of the Earth parameters that have not been estimated here are taken from *Mathews et al.* [1991b]. From those frequencies, the periods  $T$  and quality factors  $Q$  can be obtained by the relation:  $\sigma = T^{-1}(1 - i/(2Q))$ . Because our estimation of  $e^f + \text{Re}(K^{CMB})$  and  $\text{Re}(K^{ICB})$  are in agreement with that of MHB, the frequencies of the RFCN and PFCN are also in agreement. However,  $\text{Im}(K^{CMB})$  and  $\text{Im}(K^{ICB})$  are different from MHB and gives rise to quality factors  $Q_{RFCN} = 13750 \pm 514$  and  $Q_{PFCN} = 271 \pm 22$ . The values of the quality factors

obtained by MHB from their values of the geophysical parameters and equation (33) are  $18874 \pm 1395$  for the quality factor of the RFCN and  $643 \pm 117$  for PFCN. Our quality factors are significantly smaller than their ones.

## 8. Conclusion

[98] One important feature of the IAU2000 nutation model is that it is a semianalytical model, in which some Earth interior parameters are adjusted to the nutation observations. This paper presents a new method to inverse the nutation observations in order to estimate these Earth parameters. The two main aspects of this inversion are that, first, the VLBI nutation data are used directly in the time domain, avoiding the loss of information which occurs when only the first main terms in frequency are used, and, second, the Bayesian inversion method avoids linearization of the highly nonlinear nutation model. Moreover, because of several imperfections in the nutation model, we consider this model as probabilistic rather than deterministic and assume that the uncertainty on the model is Gaussian with a constant variance in time. This unknown variance is estimated from the observations jointly with the geophysical parameters.

[99] The main result is that the geophysical parameters can actually be estimated directly from the VLBI nutation time series: the intermediary step performed in MHB which consists in estimating the amplitudes of the main nutation terms in frequency can be avoided. In most cases, our estimation of the parameters have smaller standard deviations than MHB except for the parameters related to the ICB what seems to be reasonable.

[100] Some estimated parameters value are in agreement with MHB while others are not. The most different parameter is the imaginary part of the coupling constant at the ICB,  $\text{Im}(K^{ICB})$ , which is more than two times larger (in absolute value) in this paper. The differences between our estimation and that of MHB are due to the different inversion strategy, to the additional seven years of data (MHB used data until November 1999) and to empirical parameters introduced in MHB (e.g., the 0.7 factor in the ocean tide currents contribution) which are not physically justified so that we did not include them in our computation.

[101] The geophysical parameters estimated by MHB and, in particular, the core-mantle and fluid core-inner core coupling constants, have been used to infer properties of the deep interior of the Earth [*Buffett et al.*, 2002; *Mathews and Guo*, 2005; *Deleplace and Cardin*, 2006]. This paper gives a new estimation of these parameters from more recent data. The parameters which are in agreement with MHB can probably be considered as reliable but the others, in particular  $\text{Im}(K^{ICB})$ , should be used with some care when inferring physical properties of the Earth interior.

[102] **Acknowledgments.** L. Koot is a Research Fellow of the National Fund for Scientific Research (FNRS), Belgium. A. Rivoldini acknowledges the support of the Belgian Science Policy Office (PRODEX). Part of the work of O. de Viron was financially supported by the Belgian Service Public Fédéral de Programmation Politique Scientifique. The contribution of O. de Viron to this paper is IGP contribution 2335. We acknowledge the reviewers, T. A. Herring and R. Gross, for their useful comments which helped us to improve the paper.

## References

- Bizouard, C., A. Brzezinski, and S. Petrov (1998), Diurnal atmospheric forcing and temporal variations of the nutation amplitudes, *J. Geod.*, *72*, 561–577.
- Bretagnon, P., G. Francou, P. Rocher, and J. L. Simon (1998), SMART97: A new solution for the rotation of the rigid Earth, *Astron. Astrophys.*, *329*, 329–338.
- Buffett, B. A., P. M. Mathews, and T. A. Herring (2002), Modeling of nutation and precession: Effect of electromagnetic coupling, *J. Geophys. Res.*, *107*(B4), 2070, doi:10.1029/2000JB000056.
- Chao, B. F., R. D. Ray, J. M. Gipson, G. D. Egbert, and C. Ma (1996), Diurnal/semidiurnal polar motion excited by oceanic tidal angular momentum, *J. Geophys. Res.*, *101*, 20,151–20,163.
- Deleplace, B., and P. Cardin (2006), Viscomagnetic torque at the core-mantle boundary, *Geophys. J. Int.*, *167*, 557–566.
- Dziewonski, A. M., and D. L. Anderson (1981), Preliminary reference Earth model, *Phys. Earth Planet. Inter.*, *25*, 297–356.
- Gregory, P. (2005), *Bayes Logical Data Analysis for the Physical Sciences*, Cambridge Univ. Press, New York.
- Hastings, W. K. (1970), Monte Carlo sampling methods using Markov chains and their applications, *Biometrika*, *57*, 97–109.
- Herring, T. A., J. Davis, and I. Shapiro (1990), Geodesy by radio interferometry: The application of Kalman filtering to the analysis of very long baseline interferometry data, *J. Geophys. Res.*, *95*(B8), 12,561–12,581.
- Herring, T. A., B. Buffett, P. Mathews, and I. Shapiro (1991), Forced nutations of the Earth: Influence of inner core dynamics: 3. Very long interferometry data analysis, *J. Geophys. Res.*, *96*(B5), 8259–8273.
- Herring, T. A., P. M. Mathews, and B. A. Buffett (2002), Modeling of nutation and precession: Very long baseline interferometry results, *J. Geophys. Res.*, *107*(B4), 2069, doi:10.1029/2001JB000165.
- Krasinski, G. A. (2006), Numerical theory of rotation of the deformable Earth with the two-layer fluid core. part I: Mathematical model, *Celestial Mech. Dyn. Astron.*, *96*, 169–217.
- Krasinski, G. A., and M. V. Vasilyev (2006), Numerical theory of rotation of the deformable Earth with the two-layer fluid core. part II: Fitting to VLBI data, *Celestial Mech. Dyn. Astron.*, *96*, 219–237.
- Lambert, S. B. (2006), Atmospheric excitation of the Earth's free core nutation (Research Note), *Astron. Astrophys.*, *457*, 717–720.
- Lambert, S. B., and P. M. Mathews (2006), Second-order torque on the tidal redistribution and the Earth's rotation, *Astron. Astrophys.*, *453*, 363–369.
- Mathews, P. M., and J. Y. Guo (2005), Viscoelectromagnetic coupling in precession-nutation theory, *J. Geophys. Res.*, *110*, B02402, doi:10.1029/2003JB002915.
- Mathews, P. M., B. A. Buffett, T. A. Herring, and I. I. Shapiro (1991a), Forced nutations of the Earth: Influence of inner core dynamics: 1. Theory, *J. Geophys. Res.*, *96*, 8219–8242.
- Mathews, P. M., B. A. Buffett, T. A. Herring, and I. I. Shapiro (1991b), Forced nutations of the Earth: Influence of inner core dynamics: 2. Numerical results and comparisons, *J. Geophys. Res.*, *96*, 8243–8257.
- Mathews, P. M., T. A. Herring, and B. A. Buffett (2002), Modeling of nutation and precession: New nutation series for nonrigid Earth and insights into the Earth's interior, *J. Geophys. Res.*, *107*(B4), 2068, doi:10.1029/2001JB000390.
- Metropolis, N., A. W. Rosenbluth, M. N. Rosenbluth, A. H. Teller, and E. Teller (1953), Equations of state calculations by fast computing machine, *J. Chem. Phys.*, *21*, 1087–1091.
- Roosbeek, F., and V. Dehant (1998), RDAN97: An analytical development of rigid Earth nutation series using torque approach, *Celestial Mech.*, *70*, 215–253.
- Sasao, T., and J. M. Wahr (1981), An excitation mechanism for the free core nutation, *Geophys. J. R. Astron. Soc.*, *64*, 729–746.
- Sasao, T., S. Okubo, and M. Saito (1980), A simple theory on the dynamical effects of a stratified fluid core upon nutational motion of the Earth, in *Proceedings of IAU Symposium 78*, edited by E. P. Federov, M. L. Smith, and P. L. Bender, pp. 165–183, SAO/NASA Astrophys. Data Syst.
- Simon, J. L., P. Bretagnon, J. Chapront, M. Chapront-Touzé, G. Francou, and J. Laskar (1994), Numerical expressions for precession formulae and mean elements for the Moon and planets, *Astron. Astrophys.*, *282*, 663–683.
- Tarantola, A. (2005), Inverse problem theory and methods for model parameter estimation, *Soc. Ind. Appl. Math.* (SIAM).
- Wahr, J. M. (1981), Body tides on an elliptical, rotating, elastic and oceanless Earth, *Geophys. J. R. Astron. Soc.*, *64*, 677–703.
- Wahr, J. M., and Z. Bergen (1986), The effects of mantle anelasticity on nutations, Earth tides, and tidal variations in the rotation rate, *Geophys. J. R. Astron. Soc.*, *87*, 633–668.
- Wahr, J. M., and T. Sasao (1981), A diurnal resonance in the ocean tide and in the Earth's load response due to the resonant free “core nutation”, *Geophys. J. R. Astron. Soc.*, *64*, 747–765.
- Williams, J. G. (1994), Contributions to the Earth's obliquity rate, precession, and nutation, *Astron. J.*, *108*, 2, 711–724.
- Yseboodt, M., O. de Viron, T. M. Chin, and V. Dehant (2002), Atmospheric excitation of the Earth's nutation: Comparison of different atmospheric models, *J. Geophys. Res.*, *107*(B2), 2036, doi:10.1029/2000JB000042.

V. Dehant, L. Koot, and A. Rivoldini, Department of Reference Systems and Geodynamics, Royal Observatory of Belgium, Avenue Circulaire 3, B-1180 Brussels, Belgium. (laurence.koot@oma.be)

O. de Viron, Université Paris Diderot - Institut de Physique du Globe de Paris, Géophysique spatiale et planétaire-Batiment Lamarck, Case 7011, 5 rue Thomas Mann, 75205 Paris Cedex 13, France.